NASA-TM-111563

Thermal desorption of CO and H_2 from degassed 304 and 347 stainless steel

S. Rezaie-Serej
Department of Physics, Old Dominion University, Norfolk, Virginia 23529

R. A. Outlaw
NASA Langley Research Center, Hampton, Virginia 23665

(Received 23 February 1994; accepted 16 April 1994)

Thermal desorption spectroscopy (TDS), along with Auger electron spectroscopy, was used to study the desorption of H_2 and CO from baked 304 and 347 stainless-steel samples exposed only to residual gases. Both 347 and 304 samples gave identical TDS spectra. The spectra for CO contained a sharp leading peak centered in the temperature range 410–440 °C and an exponentially increasing part for temperatures higher than 500 °C, with a small peak around 600 °C appearing as a shoulder. The leading peak followed a second-order desorption behavior with an activation energy of 28±2 kcal/mol, suggesting that the rate-limiting step for this peak is most likely a surface reaction that produces the CO molecules in the surface layer. The amount of desorbed CO corresponding to this peak was $\sim 0.5\times10^{14}$ molecules/cm^2. The exponentially rising part of the CO spectrum appeared to originate from a bulk diffusion process. The TDS spectrum for H_2 consisted of a main peak centered also in the temperature range 410–440 °C, with two small peaks appearing as shoulders at ~500 and 650 °C. The main peak in this case also displayed a second-order behavior with an activation energy of 14±2 kcal/mol. The amount of desorbed H_2, $\sim 1.9\times10^{15}$ molecules/cm^2, appeared to be independent of the concentration of hydrogen in the bulk, indicating that the majority of the desorbed H_2 originated from the surface layer.

I. INTRODUCTION

Outgassing of vacuum chamber materials is of major concern in laboratory systems, deposition systems, storage rings,[1] and fusion devices,[2] especially where desorption can be further expedited by particle bombardment. Outgassing is also of concern in high-purity gas handling systems where the desorbing species introduce contamination into the gas.[3] Stainless-steel type 304, as well as type 347, are widely used in the fabrication of ultrahigh vacuum (UHV) systems primarily because of their low outgassing rate and corrosion resistance. Adams[4] has reviewed numerous studies of outgassing and adsorption–desorption properties of stainless-steel surfaces. In general, these studies have shown that the outgassing species are primarily hydrogen, carbon monoxide, water, methane, and carbon dioxide. Water is the dominant desorbing gas for unbaked surfaces, and hydrogen is the dominant gas for baked surfaces. Although there are some classic outgassing studies on stainless steel such as Calder and Lewin,[5] very few thermal desorption studies of stainless-steel surfaces have been reported.[6,7] The study by Mathewson *et al.*[6] is the only work on baked stainless-steel surfaces, which merely addresses the thermal desorption of carbon monoxide. Insufficient information still exists on the amount and kind of gases that desorb from baked stainless-steel surfaces and on details of the mechanisms by which the outgassing species are generated and desorbed.

In this work we have used thermal desorption spectroscopy (TDS) to study the desorption of hydrogen and carbon monoxide from baked stainless steels of types 347 and 304, representing the chamber wall of a typical UHV system. We have also used Auger electron spectroscopy (AES) to characterize the surfaces of these materials as a function of temperature.

II. EXPERIMENT

The experiments for this study were performed in a stainless-steel UHV system equipped with a quadrupole mass spectrometer (EAI model 250) and a calibrated Bayard–Alpert ionization gauge. The system was pumped with turbomolecular, ion, and Ti sublimation pumps to a base pressure of 2×10^{-10} Torr, with H_2 and CO as the principal residual gases.

The samples were disks of ~1 cm in diameter and 1 mm thick, machined from bulk stocks of stainless-steel types 347 and 304. They were mechanically polished with silicon carbide papers in water down to grit size 500. Before insertion into the UHV system each sample was cleaned ultrasonically in detergent (alconox) and de-ionized water, rinsed in de-ionized water, then rinsed with ethanol, and finally dried in hot air. The UHV system was equipped with a sample manipulator consisting of two Cu sample supports which facilitated the heating and cooling of the sample. The sample was mounted to the manipulator by spot welding it on its edges to two 0.25 mm diam Ta wires which were, in turn, welded to two 3.18 mm diam Mo rods that were fixed in the Cu supports. The sample was heated by resistive heating of the Ta wires with a phase-angle-controlled SCR power controller. A chromel-alumel thermocouple was welded to the back of the sample to monitor the sample temperature. The linear heating of the sample was achieved by utilizing a temperature programmer/controller (Dimension model 8710).

Thermal desorption runs for each sample were carried out after a complete system bakeout at 250 °C for 24 h and a

 0734-2101/94/12(5)/2814/6/$1.00

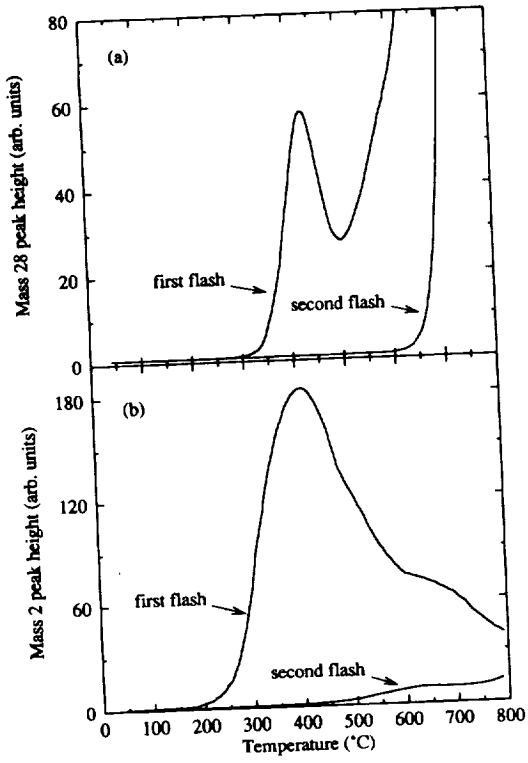

FIG. 1. Thermal desorption spectra of (a) CO and (b) H_2 from stainless steel 347 after a bakeout at 250 °C for 24 h.

subsequent 24-h exposure of the sample to the UHV residual gases. The sample was heated from room temperature to 800 °C linearly at a rate of ~3 °C/s and the resulting increase in the partial pressure of CO or H_2 was recorded as a function of temperature by a strip chart recorder. Identical TDS runs were also carried out with thin stainless-steel samples (50 mm×5 mm×0.15 mm) and a quartz cone shielding the ionizer region of the mass spectrometer in the line-of-sight geometry[8] to discriminate the desorption peaks that originated from the Ta wires and Cu supports. In order to ascertain that the detected desorption at mass 28 was due to CO, masses 14, 12, 16 were also monitored to rule out any contribution from nitrogen.

The pumping speed of the system was determined by measuring the characteristic time constant τ of the exponential decay of pressure after a rapid desorption of gas from a Ta filament. The average value for the pumping time constant τ in the pressure range 5×10^{-10}–5×10^{-8} Torr was 0.4 s for CO and 0.6 s for H_2. Since the heating rate for our desorption measurements was 3 °C/s, the product of the heating rate and the pumping time constant was less than 2 °C. Therefore the recorded pressure-temperature profiles during the TDS was proportional to the desorption rate.[9]

The sensitivity of the mass spectrometer for CO and H_2 was measured by admitting a known pressure of these gases into the vacuum chamber and recording the corresponding response of the mass spectrometer. This was repeated after each TDS run at several different gas pressures. The ionization gauge was calibrated for nitrogen using a spinning rotor gauge as a standard; the pressure readings for other gases were obtained by using the published sensitivity factors.[10]

Surface characterization of the samples was performed in a separate UHV system that was equipped with a single-pass, 10-keV cylindrical mirror analyzer for AES, operated at 5 keV electron beam energy and 1 μA beam current. The samples were heated using the identical procedure used in the TDS system. The surface composition of the sample before and after the system bakeout as well as after the thermal desorption was recorded.

III. RESULTS

Both 347 and 304 stainless-steel samples gave identical and reproducible TDS spectra, with only slight variations in their intensities. Over 20 TDS spectra were recorded. The desorbed gases observed were mainly H_2 and CO, along with small quantities of H_2O, CH_4 and CO_2. Figure 1 shows the TDS spectra of CO [Fig. 1(a)] and H_2 [Fig. 1(b)] for 347 stainless steel following a bakeout of 250 °C for 24 h. The desorption spectra for 304 stainless steel, following a similar bakeout, are shown in Fig. 2. The lower curve in each figure shows the thermal desorption upon the subsequent heating (second flash) of the sample following cooldown from the first flash. Each of the TDS spectra in Figs. 1 and 2 was recorded in a separate TDS run.

A. CO desorption

The desorption spectra for CO [Figs. 1(a) and 2(a)] consists of a sharp "leading" peak with its maximum in the temperature range 410–440 °C and an exponentially increasing part for temperatures higher than 500 °C. There is also a

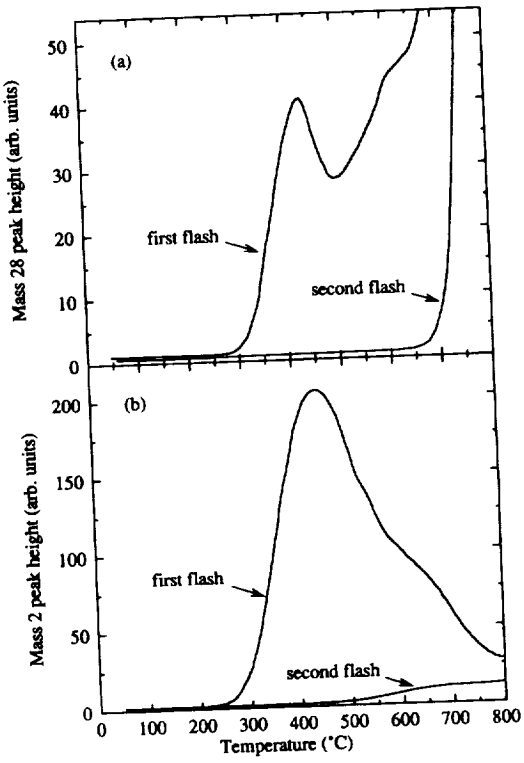

FIG. 2. Thermal desorption spectra of (a) CO and (b) H_2 from stainless steel 304 after a bakeout at 250 °C for 24 h.

small peak in the temperature range 580–610 °C which appears as a shoulder on the exponentially increasing part of the spectrum. The second flash [the lower curves in Figs. 1(a) and 2(a)] produces the same exponentially rising desorption that is observed in the first flash. Repeated flashes following the second flash produce the same desorption spectrum with progressively decreasing intensities, indicating that this exponentially rising feature is most likely due to desorption from the bulk. The CO desorption spectra presented here are in agreement qualitatively with that reported by Fujita and Homma[7] for desorption of CO from an electropolished, unbaked 304 stainless steel. The leading peak in their desorption spectrum, with a full width at half-maximum (FWHM) of ~230 °C, was centered at ~470 °C, and the shoulder peak appeared at ~690 °C, superimposed on an exponentially rising part. Contrary to this spectrum, Mathewson *et al.*[6] have observed three peaks in their spectra from a baked 304 stainless steel: a very weak peak at ~100 °C, and two broad peaks centered at 332 and 485 °C. The last peak is in good agreement with the corresponding peak in our spectra and to that of Fujita and Homma, considering the differences in the heating rates used for the thermal desorption. No desorption peak at ~332 °C was observed in our experiments; but a small peak at ~100 °C was positively identified as originating from the heating wires. Mathewson *et al.* have reported that the exponentially rising part in their desorption spectra was mainly due to the desorption of bulk nitrogen. In our spectra the exponentially rising part was definitely due to desorption of CO, as determined by monitoring the secondary peaks in the cracking pattern of CO.

The FWHM for the leading peak in our CO desorption spectra is ~105 °C. Such a narrow width suggests that this peak is a desorption peak with a single activation energy. Since this peak is separated enough from the exponentially rising part of the desorption spectrum, it may be represented by the following expression:[11]

$$R_d = -\frac{d\theta}{dt} = \nu\theta^n \exp\left(-\frac{E_d}{RT}\right), \tag{1}$$

where R_d is the rate of desorption per unit surface area, θ is the adsorbate fractional coverage, t is the time, ν is the preexponential factor, n is the order of desorption, E_d is the activation energy of desorption, R is the gas constant, and T is the temperature. If E_d and ν are coverage independent, an Arrhenius plot of $\ln(R_d/\theta^n)$ versus $1/T$ is expected to be a straight line for the correct order of the desorption reaction.[12] When the recorded thermal desorption profile is proportional to the desorption rate, the total area under a desorption peak is proportional to the initial surface coverage for that peak, and the coverage at temperature T is the total coverage minus the area integrated from the onset of the peak to temperature T. Since in our spectra only the high temperature part of the desorption peak overlaps with the exponentially rising part of the desorption spectrum, it was possible to estimate the total area under the peak and calculate the coverage in the temperature range from 340 to 488 °C by numerically integrating the desorption peak. Figure 3(a) shows the plot of $\ln(R_d/\theta^n)$ versus $1/T$ generated from the data in Fig. 1(a) for $n=2$, that is, for a second-order reaction. The

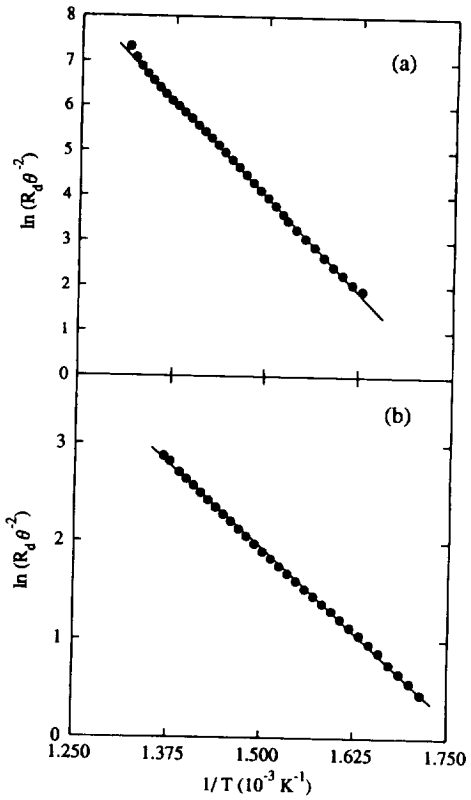

FIG. 3. Plot of $\ln(R_d/\theta^2)$ vs $1/T$ for (a) the CO desorption spectrum [Fig. 1(a)] in the temperature range from 340 to 488 °C and (b) the H_2 desorption spectrum [Fig. 1(b)] in the temperature range from 310 to 460 °C. The solid-circle data points were generated from the desorption spectra. The solid lines are linear fits to these data points.

data generated for $n=1$ (first-order reaction) do not produce a linear plot. Plots similar to Fig. 3(a) generated from the TDS spectra for all 304 and 347 samples used in this work show very good linearity and yield an activation energy of 28±2 kcal/mol. This desorption energy is higher than those reported in the literature[13,14] for the desorption of CO from stainless steel. The discrepancy may be explained on the basis of differences in the experimental conditions and the method of data analysis. Strausser[14] reported a value of 17.7 kcal/mol for the desorption of CO from a baked 304 stainless-steel surface. This value was calculated from the outgassing data collected during a cool-down period following a bakeout, where it was assumed that during this period the surface coverage would be constant. Therefore, the value reported by Strausser can only be considered as an order of magnitude for the desorption energy. In another measurement,[13] CO was adsorbed on an ion sputtered 304 stainless-steel surface. Laser-induced thermal desorption was used to study the desorption of CO. A desorption energy varying from 22 to 17 kcal/mol was calculated assuming first-order kinetics for the desorption of CO from iron which dominates the composition of a clean stainless-steel surface. However, this assumption is not well justified because both molecular and dissociative adsorptions take place on iron surfaces at room temperature.[15]

The amount of gas desorbed during thermal desorption

can be calculated from the following relation:[11]

$$N=\frac{V}{AkT_0\tau}\int_0^\infty \Delta P\, dt, \tag{2}$$

where N is the number of particles per unit surface area of the sample, ΔP is the pressure increase resulting from desorption, τ is the characteristic pumping time (volume/pumping speed) of the system, V is the volume of the system, A is the surface area of the sample, k is Boltzmann's constant, and T_0 is room temperature. Using the above relation, the amount of desorbed CO gas corresponding to the leading peak in the thermal desorption spectra was calculated to be $\sim 0.5\times10^{14}$ molecules/cm^2 of the sample geometrical surface area. This value is much smaller than monolayer quantities, supporting the fact that the CO desorption corresponding to the this desorption peak is originating from the surface layer on stainless steel.

In a recent study[16] of the removal of CO from 304 stainless steel by argon glow discharge, it has been shown that the CO removal is desorption controlled in the initial part of the glow discharge and diffusion controlled in the later part. This seems to be in accord with our desorption spectra: the sharp leading peak observed in the temperature range 410–440 °C corresponds to the desorption controlled part of the CO removal process, and the exponentially rising part corresponds to the diffusion controlled part of the process. The initial coverage of CO on a polished, baked surface has been estimated to be 1.8×10^{14} molecules/cm^2 in the above study, which compares well with our estimated value of 0.5×10^{14} molecules/cm^2; the difference between the two values may well be due to differences in sample pretreatment and bakeout, which were not reported.

B. H_2 desorption

The desorption spectra for H_2 [Figs. 1(b) and 2(b)] consist of a main peak that starts at ~190 °C and reaches its maximum at a temperature between 410 and 440 °C with a FWHM of 195 °C. There are also two shoulder peaks at ~500 and 650 °C which are superimposed on the main peak. A slowly rising component is also present, as evidenced by the second flash spectra. This component appears to be due to the diffusion of hydrogen from the bulk since successive flashes following the second flash give rise to progressively decreasing intensities for hydrogen desorption. Fujita and Homma[7] have observed three peaks at 500, 605, and 650 °C along with an exponentially rising component for the desorption of H_2 from an electropolished, unbaked 304 stainless steel. These features are again qualitatively in agreement with those in our spectra. No H_2 thermal desorption data for baked stainless steels were found in the literature. It appears that the majority of the desorbed H_2 in the TDS spectra reported here, i.e., the desorption corresponding to the main peak, originates from the oxide layer that is present on the surface before flashing the sample to 800 °C. This is supported by the fact that when the sample was subjected to a repeat of the same polishing, degreasing, and bakeout procedure (as outlined in the previous section) before each TDS run, the successive TDS runs from the same sample produced identical spectra without any decrease in the intensity.

Since a large portion of the main desorption peak is isolated from other features of the spectra, it was possible to use the same analysis method that was used for the analysis of CO desorption peak, as outlined in the previous section, to determine the activation energy of desorption and order of desorption. A plot of $\ln(R_d/\theta^n)$ versus $1/T$, as shown in Fig. 3(b), in the temperature range from 310 to 460 °C showed good linearity for $n=2$, i.e., for a second-order reaction, and yielded a value of 14 ± 2 kcal/mol for the mean activation energy of desorption. From this value the estimated activation energy of desorption per hydrogen atom is 7 ± 2 kcal/mol which is substantially smaller than the activation energy for bulk diffusion of hydrogen in 347 stainless steel: 11.5 kcal/mol.[17] This is, further, in accord with the observation that the main desorption peak originates from the surface oxide layer.

The total amount of desorbed H_2 gas was $\sim1.9\times10^{15}$ molecules/cm^2 of the geometrical area. This value is approximately equivalent to one monolayer, considering the fact that surface roughness can be as high as 2.4.[18] This again indicates that the hydrogen desorption originates from the surface layer on stainless steel, with only small contributions from the bulk diffusion.

C. Surface characterization

The composition of stainless-steel surfaces changes drastically with temperature.[17] Figure 4 shows the Auger spectra of one of our 347 stainless-steel samples at different stages before and after a thermal desorption run. The spectrum obtained before the bakeout [Fig. 4(a)] is dominated by peaks corresponding to carbon, oxygen, and iron. The surface layer in this case consists of oxides and possibly hydroxides of iron and chromium covered with a carbon contamination and traces of chlorine. The oxygen signal is partly due to the oxygen in the oxides and partly due to the oxygen in water and hydroxides. After the vacuum bakeout [Fig. 4(b)] the surface is heavily covered with carbon. The chromium concentration has increased substantially and the iron peaks have disappeared from the spectrum. This suggests that during the bakeout, as the water and hydroxides are removed, chromium diffuses to the surface and forms Cr_2O_3. This is consistent with the work of Park *et al.*[19] who, using soft x-ray appearance potential spectroscopy, observed an increase in the characteristic spectrum of this oxide after a bakeout at 200 °C. After the sample is heated to 800 °C [Fig. 4(c)] the carbon layer and oxygen virtually disappear due to desorption of CO and incorporation of carbon and oxygen into the bulk. Subsequently, the available surface sites permit sulfur segregation, the iron and chromium peaks increase, and the nickel peaks become observable. Park *et al.* also have shown that the observed chromium spectrum after heating the sample to 500 °C for several hours changed to that of a pure chromium, suggesting the decomposition of this oxide at high temperatures.

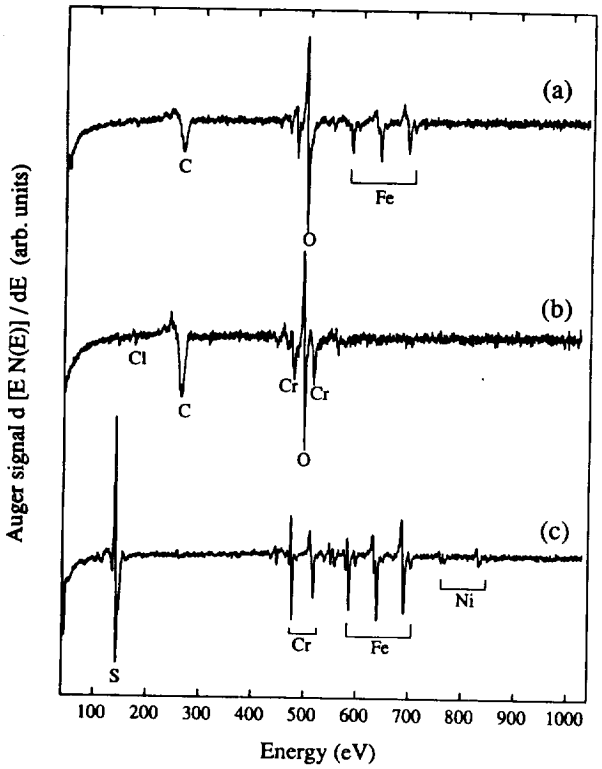

FIG. 4. Auger electron spectra from stainless steel 347; (a) before bakeout, (b) after a bakeout at 250 °C for 24 h, and (c) after heating to 800 °C at a rate of 3 °C/s.

IV. DISCUSSION

The outgassing from an unbaked stainless-steel surface is dominated by water. According to Li and Dylla,[20] this outgassing originates primarily from H_2O and H_2 sorbed in the surface oxide layer. On the other hand, the outgassing from a baked stainless-steel surface is dominated by hydrogen; the amount of desorbed hydrogen calculated from our TDS data is approximately 38 times the amount of desorbed CO.

The second-order behavior of CO desorption from stainless steel is somewhat surprising, since CO desorption is usually assumed to follow first-order kinetics.[6,13,14] However, no work in the literature could be found that addresses the kinetics of desorption of CO from a baked stainless-steel surface. The second-order behavior suggests that the rate-limiting step for the desorption is not the simple release of CO molecules from the surface, but rather a surface chemical reaction producing the CO molecules. This does not necessarily imply that the adsorption of CO on stainless steel is dissociative. There is, in fact, no reason to believe that any significant adsorption of residual CO gas takes place during or after the bakeout because the surface layer is fully oxidized. During the bakeout most of the water and hydroxides present in the oxide layer are desorbed and the surface composition is dominated by iron and chromium oxides (primarily Fe_2O_3 and Cr_2O_3) covered with a layer of carbon, as seen from the Auger spectrum in Fig. 4(b). The carbon layer is most likely due to segregation of carbon from the bulk during the bakeout. Carbon monoxide does not adsorb on Fe_2O_3,[21] and similar behavior is expected for Cr_2O_3. Further, the adsorption of CO on carbon is insignificant.[22]

The exponentially rising part of the CO desorption is probably caused by the reaction of carbon that diffuses from the bulk at elevated temperatures with oxygen from oxides in the surface layer as well as with oxygen that possibly diffuses also from the bulk.

The main peak in the H_2 TDS spectra also follows a second-order kinetics which suggests that the rate-limiting step for this peak is the formation of H_2 molecules in the surface layer from the atomic hydrogen present in the oxide layer. The contribution of bulk diffusion of hydrogen is much smaller than the contribution of hydrogen from the oxide layer, since the intensity of the desorption peak is independent of the number of times a sample is subjected to heating to 800 °C. In other words, the desorption is almost the same even from a sample devoid of bulk hydrogen.

V. CONCLUSION

Both 304 and 347 stainless-steel surfaces that have been subjected to a vacuum bakeout gave identical TDS spectra for H_2 and CO. The amount of desorbed gases corresponding to the leading peaks in these spectra was $\sim 0.5\times10^{14}$ carbon monoxide molecules and 1.9×10^{15} hydrogen molecules/cm^2 of the geometrical surface area. These values suggest that the desorbed gases originate mainly from the surface layer, with possible small contributions from the bulk diffusion in the case of hydrogen. This is further supported by the observation that the amount of desorbed H_2 was almost independent of the concentration of hydrogen in the bulk. The leading CO desorption peak displayed a second-order desorption behavior with an activation energy of 28 ± 2 kcal/mol, suggesting that the rate-limiting step in the desorption of CO is most likely a surface chemical reaction that produces the CO molecules in the surface layer. The TDS spectrum of CO included an exponentially rising part for temperatures higher than 500 °C which most likely stems from a bulk diffusion process that persists with a decreasing intensity even after repeated heating of the sample to 800 °C. This is probably caused by the diffusion of carbon from the bulk and formation of CO in the surface layer. The main H_2 desorption peak also displayed a second-order desorption behavior with a mean activation energy of 14 ± 2 kcal/mol, which suggests the rate-limiting step for this peak is the formation of H_2 molecules on the surface from atomic hydrogen present in the surface oxide layer.

ACKNOWLEDGMENT

The authors would like to thank Dr. Stuart J. Hoekje for his assistance in conducting the AES experiments.

[1] A. G. Mathewson, Vacuum **44**, 479 (1993).
[2] H. F. Dylla, J. Nucl. Mater. **93/94**, 61 (1980).
[3] F. Simondet, C. di Giulio, A. Noel, E. Ollivier, and H. de Rugy, Surf. Interface Anal. **11**, 366 (1988).
[4] R. O. Adams, J. Vac. Sci. Technol. A **1**, 12 (1983).
[5] R. Calder and G. Lewin, Brit. J. Appl. Phys. **18**, 1459 (1967).
[6] A. Mathewson, R. Calder, A. Grillot, and P. Verbeek, Proceedings of the Seventh International Vacuum Congr. and Third International Conference on Solid Surfaces, Vienna, Austria, 1977 (unpublished), p. 1027.

[7]D. Fujita and T. Homma, J. Vac. Sci. Technol. A **6**, 230 (1988).
[8]P. Feulner and D. Menzel, J. Vac. Sci. Technol. **17**, 662 (1980).
[9]C.-M. Chan and W. H. Weinberg, Appl. Surf. Sci. **1**, 377 (1978).
[10]T. A. Flaim and P. D. Owenby, J. Vac. Sci. Technol. **8**, 661 (1971).
[11]P. A. Redhead, Vacuum **12**, 203 (1962).
[12]A. M. de Jong and J. W. Niemantsverdriet, Surf. Sci. **233**, 355 (1990).
[13]J. A. Tagle and A. Pospieszczyk, Appl. Surf. Sci. **17**, 189 (1983).
[14]Y. Strausser, Technical Report No. VR-51, Varian Associates, Palo Alto, CA.
[15]A. J. H. M. Kock and J. W. Geus, Prog. Surf. Sci. **20**, 165 (1985).
[16]S. Anjali, S. V. Gogawale, and D. Ramanathan, Vacuum **44**, 837 (1993).
[17]R. A. Outlaw and D. T. Peterson, Metall. Trans. A **14A**, 1869 (1983).
[18]M. Troy and J. P. Wightman, J. Vac. Sci. Technol. **8**, 515 (1971).
[19]R. L. Park, J. E. Houston, and D. G. Schreiner, J. Vac. Sci. Technol. **9**, 1023 (1972).
[20]M. Li and H. F. Dylla, J. Vac. Sci. Technol. A **11**, 1702 (1993).
[21]G. Blyholder and E. A. Richardson, J. Phys. Chem. **66**, 2597 (1962).
[22]S. Kato, K. Josek, and E. Taglauer, Vacuum **42**, 253 (1991).